Size selective fishing: The effect of size selectivity on the equilibrium yield in the Nile perch fishery of Lake Victoria

Johannes Kammerer

Santiago Gomez-Cardona

Chrisphine Nyamweya

Size selective fishing: The effect of size selectivity on the equilibrium yield in the Nile perch fishery of Lake Victoria

Johannes Kammerer[1], Santiago Gomez-Cardona[2], Chrisphine Nyamweya[3]

October 19, 2022

Abstract

The Nile perch fishery of Lake Victoria is regulated with a slot size and with restrictions on legal gear sizes. This study provides an assessment of the effectiveness of the the slot size regulation by simulating the Nile perch fishery with a size structured population model where the size preference of the fishery is an input into the model. The model is compared to the size structure of the Nile perch population from three empirical surveys to find agreement between the model, the bottom-trawl and the catch assessment survey, while the hydroacoustic survey predicts a different population structure. The empirical fishing mortality is 2.0% above the value that produces the maximum sustainable yield, given the empirical fishing fleet selectivity. Next to the actual fleet selectivity, three alternatives are simulated to quantify the effect of the selectivity. We find that the annual yield could be increased by 17.7% by sparing fish below 50cm.

Keywords: Nile perch, size-structured population model, maximum sustainable yield, fleet selectivity, slot size

[1]Institute of Applied Mathematics, Heidelberg University, Germany

[2]Alfred Weber Institute for Economics, Heidelberg University, Heidelberg, Germany

[3]Kenya Marine and Fisheries Research Institute, P.O. Box 1881-40100, Kisumu, Kenya

1 Introduction

The size structure plays a significant role in the assessment of a fish stock and the sustainability of its fishery. The size structure describes the relative frequency of the fish sizes in the population. For fish, age and size are tightly coupled - even so far that a population can be described equivalently by the age or the size structure. Only fish of a certain size are mature and can reproduce; those play a crucial role for the reproductive capacity of the population. Additionally, the fecundity increases strongly with weight, therefore the oldest (and largest) fish have the highest per-fish contribution to the reproduction (Barneche et al., 2018; Andersen, 2020). At the same time, their percentage in the population is so low that the bulk of the spawning stock biomass consists of medium-sizes fish (Andersen et al., 2019). Every fishery needs to optimize the trade-off between maintaining the reproductive capacity of the stock (conserving large fish) and allowing the juveniles to reach the reproductive state (conserving the young fish). If the fishery threatens the reproductive capacity of the stock, one speaks of "recruitment overfishing", while fishing juveniles before they reach the economically most efficient size is called "growth overfishing" (Diekert, 2012).

In Lake Victoria (LV), a slot size regulation of 50 to 85cm was introduced ostensibly to protect immature fish, harvest mature individuals and at the same time protect the larger females (Njiru et al., 2009). The inception of slot size restrictions led to the landing of bigger-sized fish but resulted in a drastic decrease in the spawning stock biomass (Nyamweya et al., 2012). However, the upper slot size limit was lifted in the lake's Ugandan and Tanzania parts, potentially threatening the large individuals (super spawners) which are fished for fish maws (Brierley, 2018). These recent actions require assessments of the importance of the higher reproductive value of large fish in Lake Victoria.

The investigation of the selectivity of the gear types used in the Nile perch fishery

provides the possibility to use the model to simulate the effect of different fishing policies. While policymakers often know the ideal outcome, they have few tools to forcast the effect of gear type restrictions on the stock and on the reproductive capacity of the stock. The simulations thus provide a quantitative basis for policymakers to better understand the trade-off between conserving the old, fecund population and sparing the young fish to maintain the reproductive capacity for the future. Optimizing the maximum sustainable yield (MSY) in the simulation can point to the optimal use and combination of gear types to catch fish of a high value (weight or price) while maintaining the crucial capacity of the stock to regenerate.

Nile perch (Lates niloticus; 52% of LV fisheries' beach value in 2015; LVFO, 2016) and the silver cyprinid dagaa (Rastrineobola argentea; 32% of beach value with 65% of total landings in terms of mass) are the most important species for economic income and for food security and protein intake (LVFO, 2016; Njiru et al., 2018; Aura et al., 2020). Nile perch is the top predator in the system and feeds on dagaa and haplochromines as evidenced by stomach content analysis (Njiru et al., 2009). Certain parameters in the model which is used in this study represent characteristic features of the ecosystem, therefore this study complies with the Ecosystem Approach to Fisheries Management which has been demanded as a necessary paradigm shift for sustainable management of the African inland lakes (Musinguzi et al., 2016; Link et al., 2020).

2   Literature Review

A simple population model would deal with an unstructured population where the total biomass of the population is the main variable. With such models, Downing et al. (2013a) found that the delay of the Nile perch upsurge could come from mere logistic growth, and van de Wolfshaar et al. (2014), with an unstructured predator-

prey model, studied the imbalance between Nile perch and Haplochromines in a
cascade and a depensation scenario. As the next step in complexity one can consider
the two-stage models that distinguish between juvenile and adult fish. Using such
an approach, Downing et al. (2012) and Natugonza et al. (2016) studied the trophic
position of juvenile and adult Nile perch in the food chain of Lake Victoria through
simulations in the Ecopath framework (Christensen and Walters, 2004).

Nile perch is a species with life-history omnivory, i.e. the diet changes across
lifetime, therefore the prey size depends strongly on the life stage. Models where the
population is continuously structured in the size variable, so-called size-structured
models, are well fit to incorporate the size-dependent predator-prey relationships.
With size-structured models, Downing et al. (2013b) studied the dependency of the
Nile perch population on the resource structure, and van Zwieten et al. (2016) found
that the switch from haplochromines to a Nile perch dominated food web might
have come from a eutrophication-triggered failure in the haplochromine recruitment
rather than merely from fishing pressure or the Nile perch population alone.

This paper also uses a size-structured approach, but applies another modelling
framework to the Nile perch population. It uses the framework developed by An-
dersen (2019), where the growth and feeding equations are derived from biological
scaling laws. The framework is considered to be sound in its theoretical grounding
and through its generality flexible enough to be applied to multiple situations and
fish stocks and allows to make predictions under different fishing patterns.

In the literature, most of the MSY estimates which we found, date back to
previous decades, with the exception of Aura et al. (2020), who use survey data
from 2009-2018 to calculate the standing stock biomass of Nile perch in Lake Victoria
(553,770t in 2018) and recommend to reduce the yield by 40% to achieve MSY at
86,096 t, based on a Schaefer model. For the period 2005-07, Kayanda et al. (2009)
estimates a Y/B ratio of 0.44 at B=579kt. They use the formula $MSY = 0.5 \cdot (Y + M \cdot$

B) to estimate the MSY from data of the annual yield Y, the natural mortality M and the biomass B; they find a MSY value of 323 kt/yr (1999-2001) and 212 kt/yr (2005-2007). Kyomuhendo (2002) use an economic model to estimate the MSY and MEY from data of 1975-2000 and find MSY=306.9 kt/yr and MEY=285.9 kt/yr. Using a non-equilibrium Schaefer surplus-production model and catch-effort data, Pitcher and Bundy (1995) find, for four scenarios, MSY values between 278.6-489.0 kt/yr. For the standard effort scenario, they find the MSY between 269.6-317.6 kt/yr.

3 Model

Basic assumptions. The model is based on the following assumptions: The relevant entity in the population is the individual fish; the population dynamics follow from the life history of the individual fish. The individual fish has a bioenergetic budget; growth, reproduction and non-predation mortality rates follow from it. Fishing is a size-selective process; its targets fish in a specific size range and leads to an additional mortality. We consider the population to be in a (dynamic) equilibrium, no time-dependent processes were simulated. We study the maximum sustainable yield assuming full enforcement of the policy.

Mathematical formulation. Let $u(t,w)$ be the **population density** at time t and weight w ($u : \mathbb{R} \times [w_0, W_\infty) \to [0,\infty); w_0, W_\infty \in \mathbb{R}^+$). $u(t,w)\,dw$ is the **number of fish** in $[w, w+dw]$. Let $g(w)$ denote the size-dependent **growth rate** ($g : [w_0, W_\infty) \to (0,\infty)$). $\mu(w)$ is the **mortality** which is the sum of the biological and the fishing mortality ($\mu : [w_0, W_\infty) \to (0,\infty)$).

The evolution of the population is described by the McKendrick-von Foerster equation (McKendrick, 1925; von Foerster, 1959) with

$$\frac{\partial}{\partial t}u(t,w) + \frac{\partial}{\partial w}(g(w)u(t,w)) = -\mu(w)u(t,w) \tag{1}$$
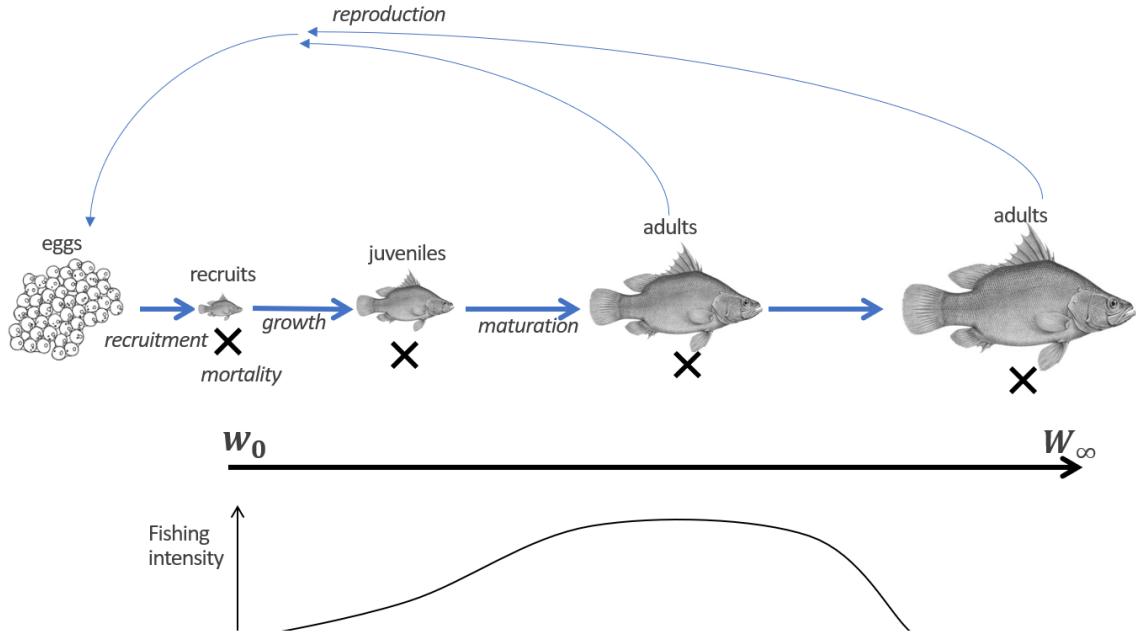
5

Figure 1: Top: size structured Nile perch model with recruitment, mortality, growth, maturation and reproduction (Andersen (2019)). Bottom: Example selectivity of the fishery.

The Dirichlet boundary condition is given by the recruitment flux f, which is a functional that can depend on the total population.

$$u(0, w) = u_0(w) \; on \; [w_0, W_\infty) \tag{2}$$

$$u(t, w_0) = f(u(t, w)) \; on \; [0, T_{max}] \tag{3}$$

In equilibrium $u(t, w)$ is replaced by $u(t)(u : [w_0, W_\infty) \to [0, \infty))$ and the ordinary differential equation can be solved readily:

$$\frac{d}{dw}(g(w)u(w)) = -\mu(w)u(w) \tag{4}$$

$$u(w_0) = f(u(w)) \tag{5}$$

$$u(w) = \frac{u(w_0)g(w_0)}{g(w)} \exp\left(-\int_{w_0}^{w} \frac{\mu(\tilde{w})}{g(\tilde{w})} d\tilde{w}\right) \tag{6}$$

The biphasic growth model (Andersen, 2019) is defined by

$$g(w) = Aw^n \left[1 - \psi_m(w) \left(\frac{w}{W_\infty} \right)^{1-n} \right] \tag{7}$$

with the growth parameter $A \in \mathbb{R}^+$, the maturation rate $\psi_m : [w_0, W_\infty) \to [0, 1]$ and the metabolic exponent $n \in \mathbb{R}^+, n \approx 3/4$.

The mortality is

$$\mu(w) = \mu_0(w) + \mu_F(w) \tag{8}$$

which is the sum of the natural mortality,

$$\mu_0 = aAw^{n-1} \tag{9}$$

with physiological mortality $a \in \mathbb{R}^+)$ and the fishing mortality

$$\mu_F = F\psi_F(w) \tag{10}$$

where $\psi_F : [w_0, W_\infty) \to [0, 1]$ denotes the fleet selectivity, and $F \in \mathbb{R}_0^+$ the fishing mortality. Then, for given F, the solution of eq. (6) is

$$u(w; F) = \frac{u(w_0)g(w_0)}{g(w)} \exp\left(- \int_{w_0}^w \frac{\mu_0(\tilde{w}) + F\psi_F(\tilde{w})}{g(\tilde{w})} d\tilde{w} \right) \tag{11}$$

Derived quantities. The following derived quantities are relevant.

Spawning stock biomass $(SSB : \mathbb{R}_0^+ \to \mathbb{R}_0^+)$

$$SSB = \int_{w_0}^{W_\infty} u(w; F)w\psi_m(w)dw \tag{12}$$

Reproductive output $(R_p : \mathbb{R}_0^+ \to \mathbb{R}_0^+)$

$$R_p = \frac{\epsilon_R}{w_0} R_{egg} SSB \tag{13}$$

Recruitment $(R : \mathbb{R}_0^+ \to \mathbb{R}_0^+, R_{max} \in \mathbb{R}_0^+)$

$$R = \frac{R_{max} R_p}{R_{max} + R_p} = u(w_0) g(w_0) \tag{14}$$

Catch distribution

$$C(w) = F u(w; F) w \psi_F(w) \tag{15}$$

Yield

$$Y(F) = F \int_{w_0}^{W_\infty} u(w; F) w \psi_F(w) dw \tag{16}$$

Maximum sustainable yield

$$MSY = \max_F Y(F) \tag{17}$$

and the fishing mortality that leads to MSY

$$F_{MSY} = \arg \max_F Y(F) \tag{18}$$

For a thorough discussion of these quantities the reader is referred to Andersen (2019). For the analysis, the integrated growth is compared to the widely used van Bertanlanffy growth equation

$$L(t) = L_\infty (1 - \exp(-K(t - t_0))) \tag{19}$$

which can be converted to weight used the weight-length relationship

$$w = cL^b \tag{20}$$

with the parameters c and b (see appendix).

4 Materials

The fisheries research institutes (NaFiRRI, TAFIRI and KMFRI) and the LVFO regularly conduct bottom trawl surveys, where measurements at up to 80 stations are taken, with a focus on shallow regions (Kayanda et al., 2009; Mgaya and Mahongo, 2017). Usually, 30-minute trawls with a trawler speed of around 2.5-3.5 knots are taken (R. Kayanda, pers. comm., Sep. 2020). The trawls are fully selective for fish from about 10cm to 40cm (Kolding et al., 2008). It is subject to a current discussion whether the trawl technique has a lower selectivity for fish larger than 40cm because they might be capable of escaping the trawl as their swimming speed is comparable to (or higher than) the trawl speed. Indeed, the number of large specimen is very low in the trawl surveys, although a few ones are caught. For more information, see Kolding et al. (2008).

Hydroacoustic surveys use underwater sound to detect, enumerate, and measure the distribution of fish (LVFO, 2019). Currently, the acoustic surveys are used to estimate fish quantities in Lake Victoria. These surveys form an important part of routine stock assessments and enable large areas to be surveyed at high spatial resolution in a relatively short period. The estimates of abundance and distribution can then be used in assessment models to provide estimates of sustainable yield (Perivolioti et al., 2020). Nile perch are strong acoustic targets, distinguishable as 'single targets' (i.e., not in schools), hence easy to assess through echo count-

9

ing. The relative strength of individual echoes is a derivative size of Nile perch (total length), which is determined using the single targets algorithm in Echoview (Echoview Software Pty Ltd., 2016) following the established target strength-total length relationship (Kayanda et al., 2012). Acoustic estimates of Nile perch size are 'ground truthed' by reference to samples obtained by trawling. However, in some years, there are discrepancies in size structures determined using the acoustics and trawling methods.

The Lake Victoria Fisheries Organization (LVFO) conducts regular Catch Assessment Surveys (CAS). Between 2005 and 2015, fifteen CAS were carried out at 143 pre-selected landing sites in Kenya, Tanzania and Uganda (LVFO, 2016). Those are approximately 10% of the landing sites at the lake. The CAS are conducted under regionally harmonised Standard Operating Procedures (SOPs). The CAS provide the partner states within the East African Community (EAC) with data monitoring the fisheries and the exploitation of the fisheries resources. They provide information about the catches, the effort, and the catch per unit of effort (CPUE). The harmonized fisheries data collection conducted by EAC through the LVFO also include bi-annual Frame Surveys (FS). In these surveys, information are collected to indicate the effects of the fisheries management and of interventions as well as baseline data for fisheries planning and development. This includes the number of landing sites, of fishers, and of gear and craft combinations by target species (LVFO, 2017). At each location, craft/gear combinations are randomly sampled by the field enumerator and field data are recorded in harmonized data forms. For each effort group (craft-gear combination), the mean fish catch rates by species (kg per boat per day) is estimated.

5   Methods

5.1   Length and weight

Most empirical spectrum measurements are designed as length measurements, e.g. bottom-trawl and hydroacoustic surveys. The spectrum in the length domain is, however, not identical to the spectrum in the weight domain, as they are related by the non-linear relationship $w = cL^b$. A mathematically derived relationship was used to convert from one to the other spectrum. It is described in the Appendix and was validated against the method LBNbiom (Edwards et al., 2017).

5.2   Fisheries Reference Points

Reference points are a measure of the resilience of a stock with respect to fishing (Andersen, 2019). They can be target points (goals) or limit points (thresholds to be avoided) and they can refer to the biomass of the stock or to the exploitation level (fishing mortality). The central reference point is the point of maximum sustainable yield, which denotes the maximal annual catch in equilibrium. The fishing mortality that corresponds to the MSY situation is denoted with F_{MSY}. A discussion of MSY, its possible problems and other reference points can be found in Andersen (2019).

5.3   Numerical equilibrium spectrum

The equilibrium of the McKendrick-von Foerster equation is calculated using the R library *fishsizespectrum* [1]. It involves a numerical discretization scheme with the following steps (Andersen, 2019):

1. the range $[w_0, W_\infty)$ is discretized into m logarithmically distributed weight classes w_i

---

[1]https://github.com/Kenhasteandersen/FishSizeSpectrum

Table 1: Parameter values.

parameter	value	interpretation
b	3.26	lenght-weight-exponent
c	0.0042	length-weight-coefficient
K	0.22	van Bertanlanffy growth constant
W_∞	60,000g	asymptotic weight
L_∞	156.6cm	asymptotic length
w_{mat}	4,380g	weight at maturation
A	13.02	growth coefficient
M	0.39/yr	adult mortality
a	0.3	physiological morality

2. at each grid point, the total mortality is calculated

3. the population density at weight w is proportional to the survival probability from w_0 to w

4. the population density can be calculated from a closed integral formula

The parameter values are shown in Tab. 1.

6   Results

In a first step, the model was validated against empirical data, in a second step the model was simulated under modified fishing intensity and thirdly, the effect of four fleet selectivity scenarios on the equilibrium yield was analyzed.

6.1   Model validation

In the first step, we found that the model reproduces the van Bertalanffy growth curve of Nile perch and that the simulated biomass spectrum is similar to bottom

trawl survey and catch assessment survey, but differs from hydroacoustic survey, as will be explained in the following.

The numerical solution of the growth equation (eq. 7) produces the curve of weight-at-age. This is compared to the classical van Bertalanffy growth curve for empirical parameters of Nile perch (Fig. 2). For young ages, both curves are flat because young fish are small and have a small growth rate. After around one year, the slope becomes steeper and reaches a maximum, where the growth rate is maximal due to large food consumption while still having moderate energy losses from reproduction and other sources. At higher ages, the curves become flatter again, until they converge to the asymptotic weight, where weight gains and losses are balanced (here 60kg). The biphasic growth curve predicts a lower weight until around 2.5 years and after around 4 years. This is also visible in the length-at-age curve (appendix). The van Bertanlanffy curve predicts higher weights because in its construction it needs, in order to fit empirical data, the parameter t_0 that is the interpreted as the "age at zero length" and has a negative value, such that the individuals' growth curve actually starts before birth. The biphasic growth model avoids this construction.

Next, the fishery was simulated in the model as the solution of eq. (11) for three levels of peak fishing mortality with the empirical fleet selectivity from Gómez-Cardona et al. (2022). As predicted from theory and observations (Andersen, 2019), the biomass spectrum is similar to a flat spectrum in the unfished part of the spectrum (solid curves in Fig. 3). The black curve represents the simulation with peak fishing mortality F=0.5/yr. At around 600g, the fishing pressure becomes stronger (as the selectivity increases), and the biomass spectrum begins to decline. It would further decline until and beyond the peak of the selectivity at 2000-3000g. However, parallel to the increase in selectivity, fish start to maturate in this range. As they become mature, they start to reproduce and put energy into reproduction which leaves less energy for growth, therefore the growth rate slows down. The fish "pile
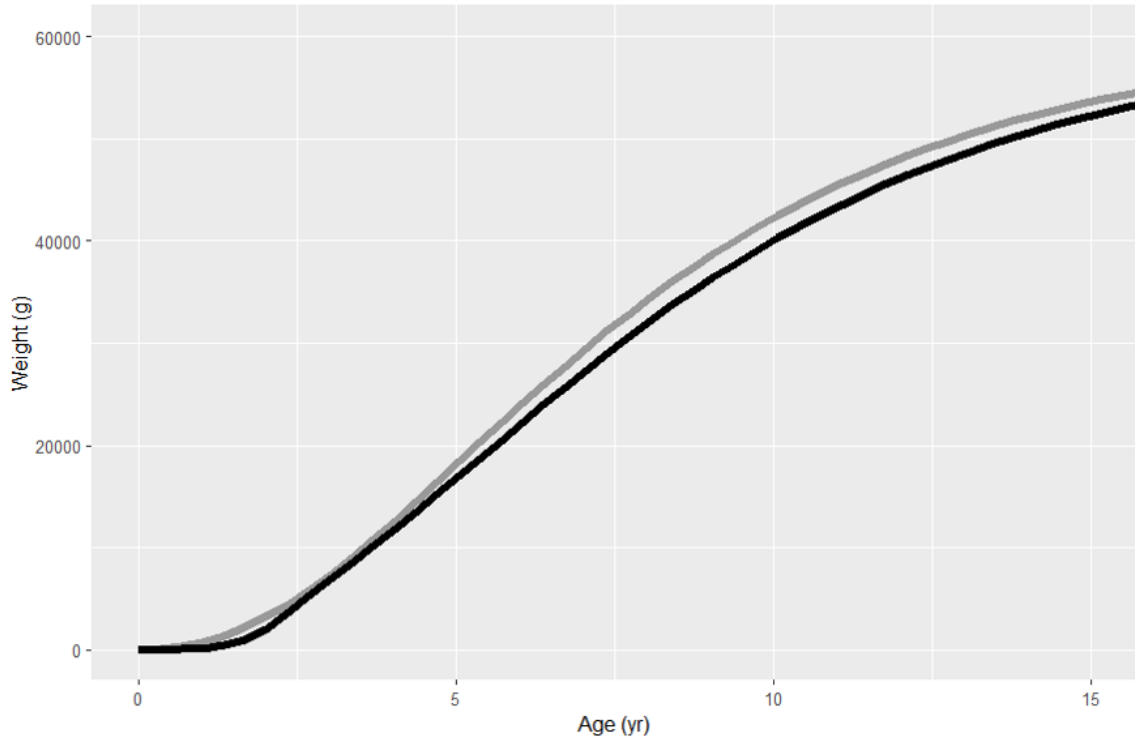
13

Figure 2: Van Bertalanffy growth curve (grey) vs integration of the differential equation dw/dt with biphasic growth (black).

up" around the point of 50% maturity (70cm or 4348g). This counteracts the fishing pressure and leads to an increasing population density in the range 3000-8000g. At around 10,000g, the growth rate has become so small that fish spend much time in each "weight bin". Therefore, the mortality rate exceeds the growth rate and thus the spectrum decreases strongly.

For a higher fishing mortality (darkgrey: 1.0/yr, grey: 1.5/yr), the biomass density descreases faster the in fished range, i.e. the slopes are more negative. At F=1.5/yr, the fishing mortality counteracts the effect of fish "piling up" around maturation, resulting in a strictly monotonous decreasing curve. The bottom trawl survey is shown for comparison (dashed in Fig. 3). It has a small negative slope until around 50cm (1,451.75g, begin of the grey rectangle that spans the range 50-85cm), where it suddenly breaks down. At this point, two effects would coincide. First, the actual decreasing population density and, secondly, the impaired selectivity of
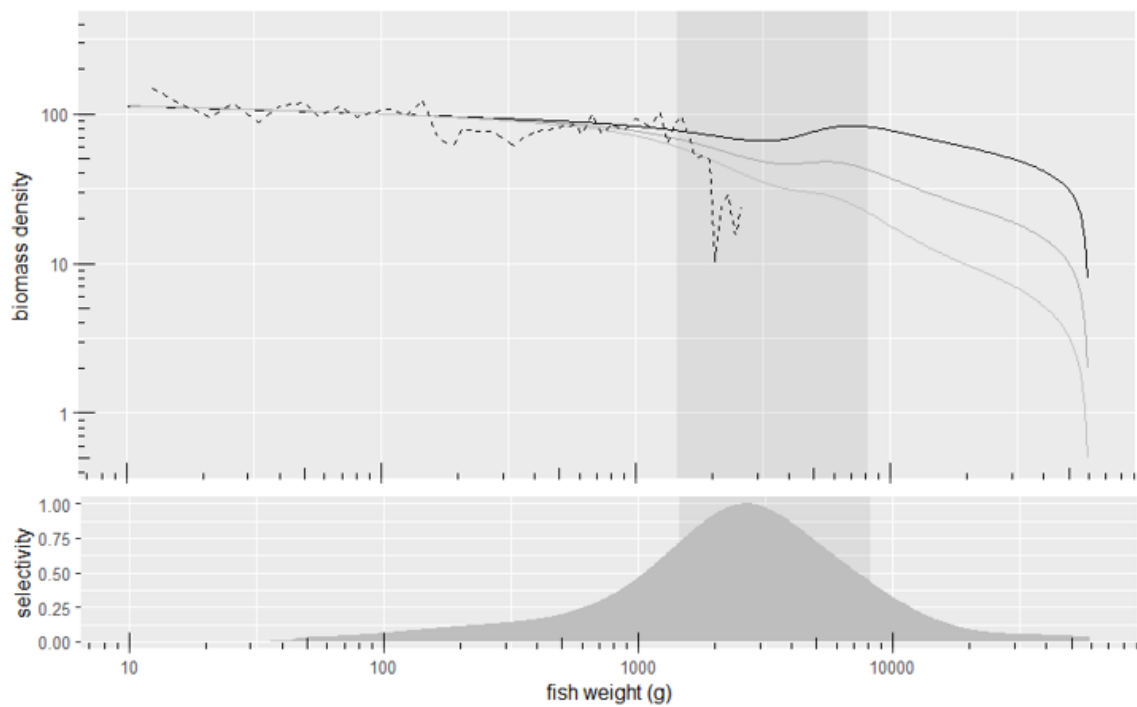
14

Figure 3: Top: bottom trawl survey (2019, dashed) compared to simulations of Nile perch biomass spectrum (solid) for F=0.5 (black), 1.0 (darkgrey) and 1.5/yr (grey). Bottom: empirical fleet selectivity (2020). Grey-shaded rectangles mark the legal slot size (50-85cm).
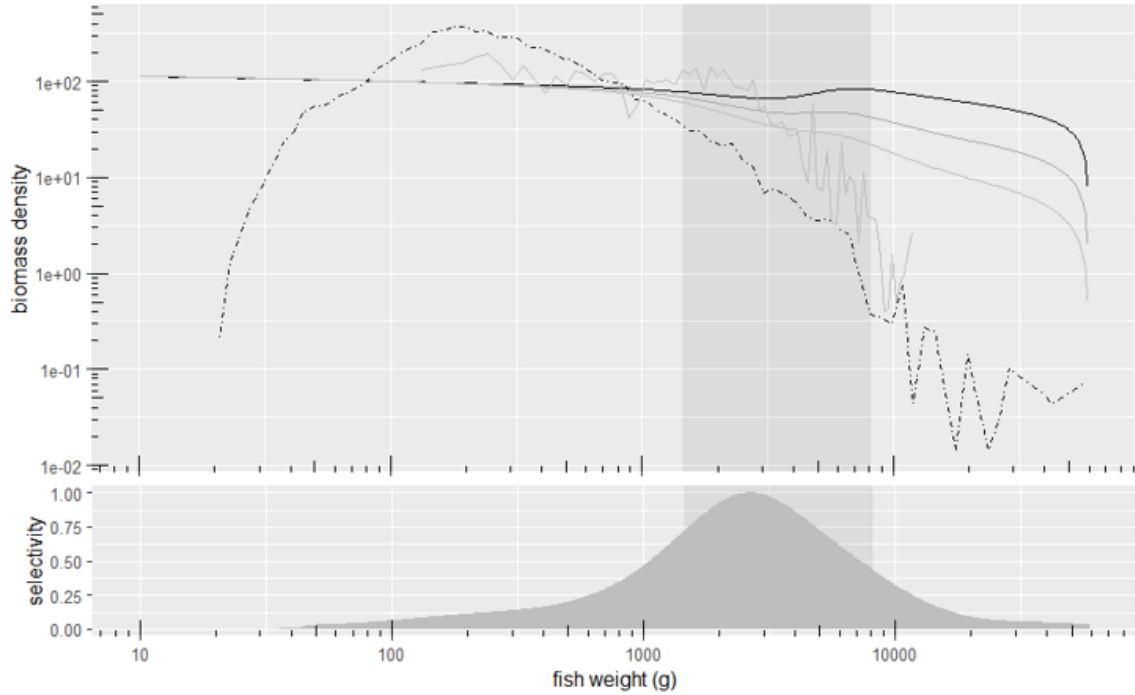
Figure 4: Top: hydroacoustic survey (2019, dotdash) and catch assessment survey (CAS, 2020, grey) compared to simulations of Nile perch biomass spectrum (solid) for F=0.5 (black), 1.0 (darkgrey) and 1.5/yr (grey). Bottom: empirical fleet selectivity (2020). Grey-shaded rectangles mark the legal slot size (50-85cm).

bottom trawl surveys for larger fish. Currently, the exact selectivity of bottom trawl
surveys, in particular the exact point at which the selectivity drops, is not studied
well enough, but future studies could provide the selectivity curve and allow to
disentangle the two effects.

In Fig. 4, the three simulations are compared with the hydroacoustic surveys
(dot-dash) and the spectrum estimate from the CAS (grey). The hydroacoustic
curve shows a different behaviour pattern that the other curves. For sizes above
200g, the slope is more negative than for CAS and the simulations. This relates
to the TS-weight conversion (see Materials). The conversion could be the reason
for a steeper slope. However, this needs further investigation to re-analyse the
hydroacoustic survey raw data. The curve of the CAS estimate is similar to the
simulations until around 3000g and afterwards it drops steeply. However, in the
CAS data there were very few observations of larger fish (above 75cm or 5444g) in

16

gillnets and few above 85cm (8188g) in longline hooks. For the latter, the catch size and hook size are only weakly correlated, therefore the hook size has only limited impact on the size of maximum selectivity. Because of the few data points of larger fish, the right part of the CAS spectrum has lower confidence.

Tab. 2 shows the sum of squared residuals (SSR) between (the logarithm of) the simulated biomass spectrum (F=1.0) and the respective survey (normalized, linearly interpolated, logarithmic, 141 data points each) over the range 200g-2500g where all are comparable. A value of zero would indicate perfect agreement, and the larger the disagreement, the larger is the SSR. It confirms that the simulation, the bottom trawl survey and the catch assessment survey agree mutually, while the hydroacoustic survey describes a very different population structure.

Table 2: Sum of squared log-residuals over 200g-2500g between the simulated biomass spectrum (F=1.0) and the respective survey (normalized, linearly interpolated, 141 data points).

survey	SSR-log
BT2019	3.385286
HA2019	51.16156
CAS2020	2.979331

6.2 Stock under modified fishing level

In addition to the population spectrum, the size distribution of the catch was simulated with eq. (15) for the three levels of fishing mortality (0.5, 1.0, 1.5/yr) which is shown in Fig. 6. The top row shows the biomass spectrum like in Fig. 3 and 4. It is scaled to be 1 at w=1mg. The bottom row of Fig. 6 displays the spectrum of the catch for the three levels of fishing mortality. Fig. 5 shows the empirical fleet selectivity which peaks at around 60.2cm (2659.2g). A major part of the selectivity curve lies left of 50cm and thus outside of the legal range (50-85cm, grey shaded
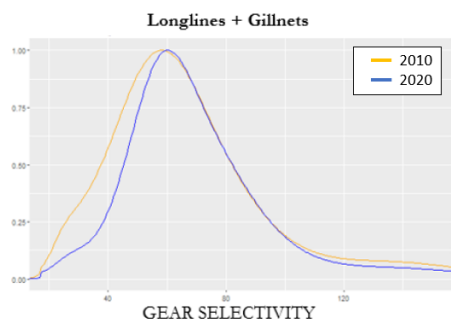
17

Figure 5: Empirical fishing fleet selectivity from catch assessments surveys. Adapted from Gómez-Cardona et al. (2022).
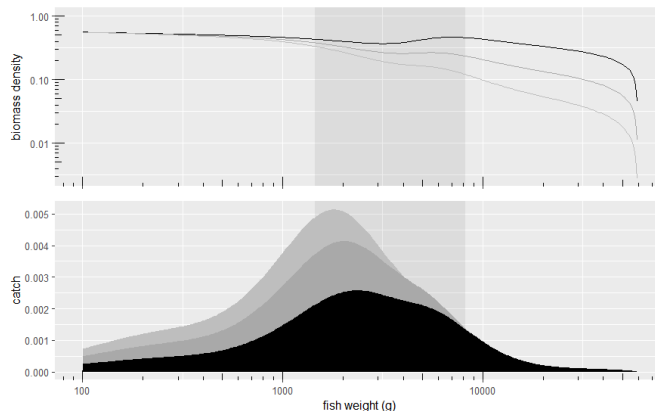

Figure 6: Simulations of Nile perch biomass spectrum (top) and catch distribution (bottom) with the empirical fleet selectivity (2020) for F=0.5 (black), 1.0 (darkgrey) and 1.5/yr (grey).

rectangle).

The following can be observed: First, the peak of the catch curve is not equal to the peak of the selectivity curve, but lies left of it. The reason is that the spectrum is declining, therefore the density of fish is higher at smaller sizes. The catch, being the product of biomass density and selectivity, is thus shifted to the left. For F=0.5/yr, where the biomass spectrum is almost flat in the legal range and even has a positive slope when fish pile up around maturation (70cm), the catch curve has, next to the peak, a second hump right of it - at the position where the biomass density has a local maximum.

Secondly, the peak of the catch spectrum moves further to the left with increasing fishing intensity, from 2388.2g (0.5/yr, black) to 1825.6g (1.5/yr, light grey). The reason is found in the biomass spectrum: for F=0.5/yr, the spectrum is almost flat up until around 10,000g. For F=1.0/yr and 1.5/yr, the spectrum declines earlier, already in the range of legal fishing, 50-85cm. Therefore, the peak catch weight moves also towards lower sizes.

Thirdly, the catch rates in the range up to around 4000g increase with increasing fishing mortality. Beyond 4000g, however, the catch rates with 1.5/yr (light grey)

are lower than the rates with 1.0/yr (grey). The reason is: under the the higher fishing pressure less fish survive such that the density of fish is now so low that it is not even compensated by the higher mortality. It is visible that a smaller fishing mortality can leads to higher catch rates of large fish (even in absolute numbers).
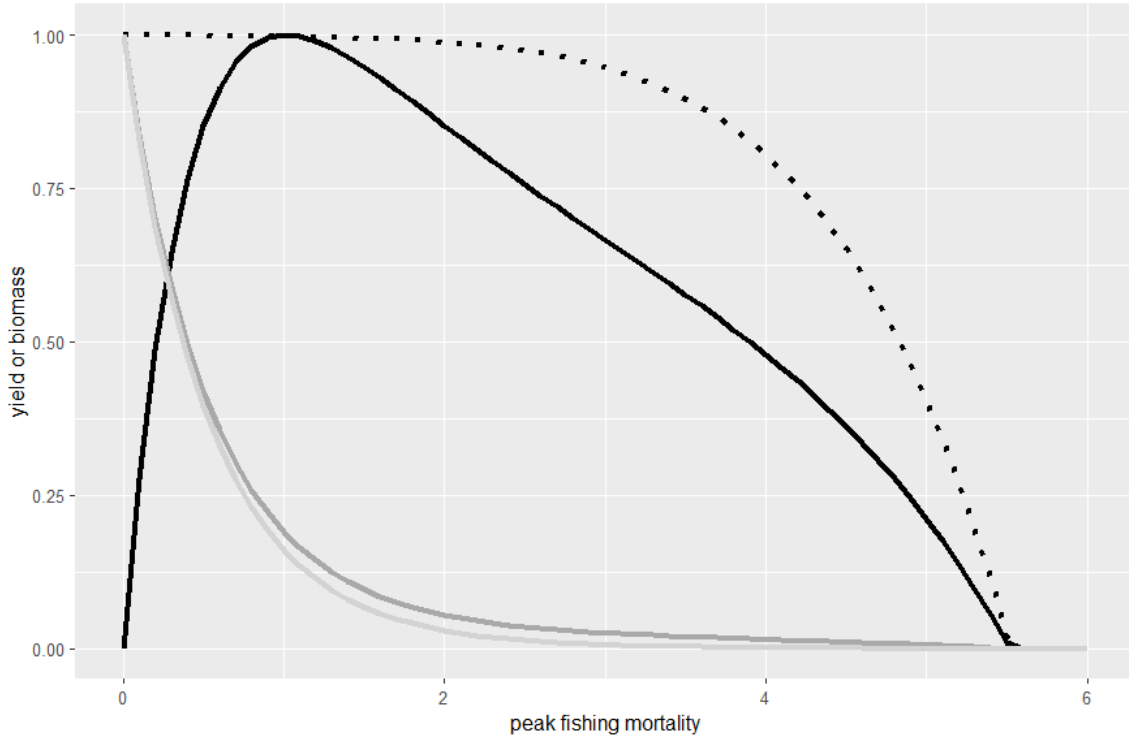

Figure 7: Fisheries characteristics for the observed fishing fleet selectivity (Gómez-Cardona et al., 2022). Black: yield biomass, darkgrey: stock biomass, lightgrey: spawning stock biomass, dotted: recruitment. All values are scaled to the maximum.

A full representation of the fishery includes both the selectivity $\psi_F(w)$ and the level (intensity) of fishing, F. While the first one has been derived from the catch assessment survey (Gómez-Cardona et al., 2022), the level can be estimated by the yield to biomass ratio. From yield and biomass data from 2014 and 2015 (LVFO, 2016, 2019), the yield-to-biomass ratio is 0.304/yr, assuming the biomass of 2015, B=683.18kt (LVFO, 2019). This is similar to the baseline (2015) fishery condition in the Atlantis (0.312/yr) and EwE (0.340/yr) simulation, respectively, of Natugonza et al. (2019); and it is lower than the value 0.44/yr, that is reported by Kayanda et al. (2009) for the period 2005-2007. Given the empirical selectivity

in the model, the yield-to-biomass 0.304/yr ratio is achieved with a peak fishing mortality F=1.035993/yr.

The fishing level comes from fishers' decisions on their individual effort, and can therefore be subject to ongoing change. To predict how the fish stock and the yield would react to various fishing levels, the fishery is simulated with eq. (11) for the range of peak fishing mortality from 0/yr to 6/yr (Fig. 7). Initially, from 0 to 1/yr, the yield increases rapidly, as fishing increases while the stock recruitment is not impaired yet. It is not impaired because the non-linearity buffers the additional fishing mortality, i.e. here fishing replaces the mortality early in life which is modelled by the non-linearity. At F=1.01523/yr, the fishery reaches the maximum sustainable yield (MSY). Between 1/yr and 4.5/yr, the yield descreases almost linearly with fishing mortality. It is remarkable that the yield at F=2/yr is still high (around 85.2% of MSY), while the SSB has already decreased to 3.0% of the unfished state. This is possible because the recruitment is still at 98.9% and it demonstrates the enormous effect (and potential) of the non-linearity in recruitment which models the density-dependent effects early in life and which is particularly strong for large fish like Nile perch (Andersen, 2019). At F=4.83/yr, the recruitment is reduced to 50% or recruitment of the unfished population. Afterwards, the yield drops quickly, and at the 5.52/yr, the stock is collapsed completely, resulting in zero recruitment, zero SSB and zero yield.

6.3 Four selectivity scenarios

We studied the effect of alternative fleet selectivities. The study is inspired by recent modifications of the legal fishing range. As we are interested only in the question how a given fleet selectivity translates into a stock size distribution, optimal fishing mortality (Fmsy), annual yield, and catch size distribution, we exclude the effects of the re-distribution of fishing pressure in the respective range of legal fishing. This
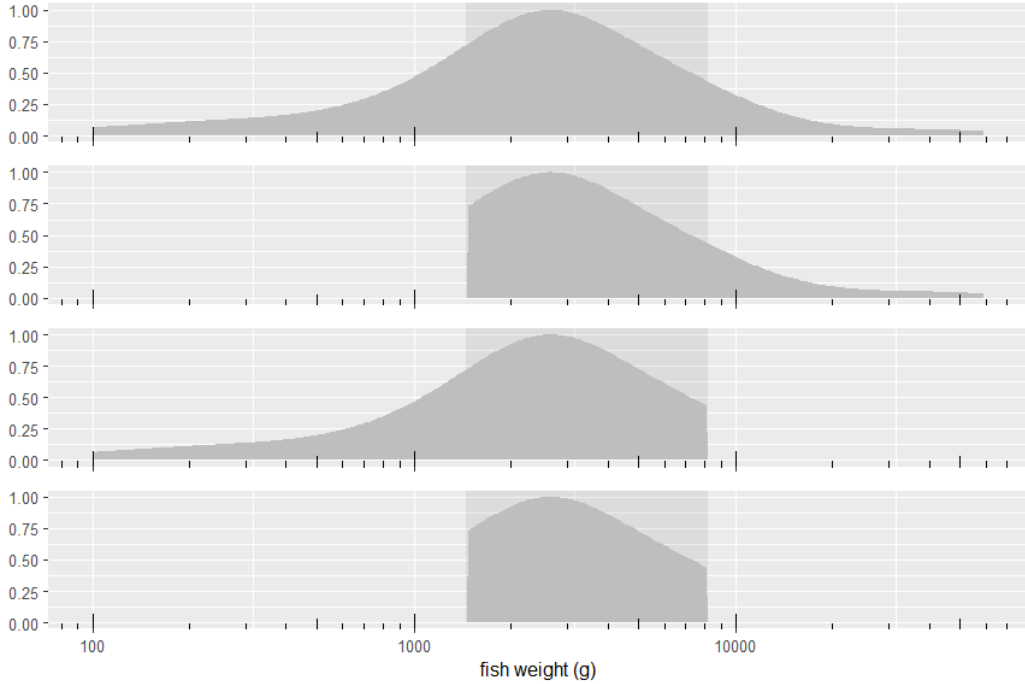
Figure 8: Top: empirical fleet selectivity (2020, Gómez-Cardona et al. (2022)). Second and third row: cropped fleet selectivities (>50cm and <85cm). Bottom: fleet selectivity within slot size (50-85cm).

means that, in each scenario, inside the respective legal range the fishing selectivity is identical to the observed selectivity, and outside of the range it is zero. By doing so, we can also study the effect of a stricter enforcement of existing size regulations.

The four scenarios are: (1) empirical fleet selectivity, (2) fishing only above 50cm, (3) fishing only below 85cm, (4) fishing only from 50-85cm (Fig. 8). The model of this study does not predict how the fishing level would adapt if the fleet selectivity were modified. Under different policy regulations or under a stricter enforcement of the bounds of the slot size, fishers' would re-distribute their fishing effort to sizes that are more profitable to them, either because of higher yield, higher per-kilo price (for larger fish) or to avoid penalties for using illegal gear sizes. The adaptation behaviour of fishers is part of future research.

The four scenarios are simulated as the solution of eq. (11) over the range of F=0 to F=6/yr. From the population and the fishing mortality, the equilibrium yield (eq. 16) was calculated across the entire range (Fig. 9). The four scenarios

21

can be compared from various perspectives: First, they can be compared at the current level of fishing mortality (black vertical line in Fig. 9). This corresponds to a situation where the fishing level of the legal range 50-85cm stays the same, but, depending on the scenario, there is no fishing below 50cm, above 85cm, or both.
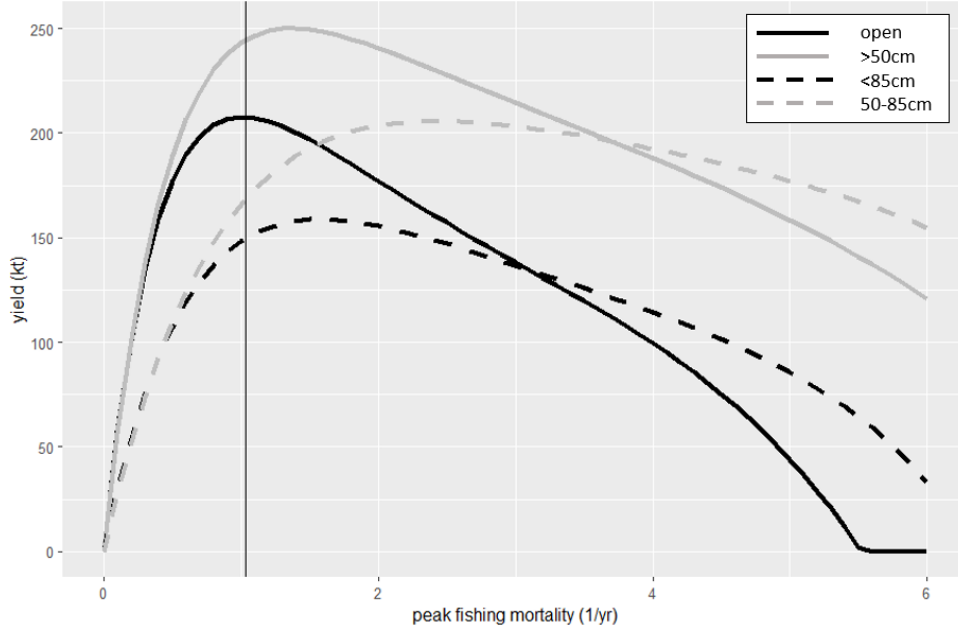

Figure 9: Yield dependent on fishing mortality for the four selectivity scenarios. The black vertical line is the empirical fishing mortality.

Table 3: Best fishing mortality F_{MSY} (1/yr), maximum sustainable yield Y_{MSY} (kt) and yield and SSB at empirical peak fishing mortality $F_{emp} = 1.035993$ (from catch and biomass data from 2014 and 2015).

scenario	Y_{Femp} (kt)	SSB_{Femp} (kt)	F_{msy} (1/yr)	Y_{msy} (kt)
open	207.5936	537.2761	1.015230	207.7713
> 50cm	244.302	701.5037	1.371135	250.0450
< 85cm	149.5158	919.8501	1.576678	158.7763
$50 - 85$cm	168.3612	1201.056	2.432108	205.6201

370 In this case, catching no fish below 50cm while keeping the fishing mortality above 50cm the same, increases the annual yield by 17.7.% from 207.5936kt to 244.302kt (Tab. 3). Catching not fish above 85cm (scenario 3), however, decreases yield by -28.0% from 207.5936kt to 149.5158kt, with scenario 4 being somewhat better, but

still below the open scenario. The SSB increases in each scenarios because the fishing

375 pressure, in total, is reduced.

Secondly, the scenarios can be compared at the fishing level, that is optimal in each respective case. This MSY level (eq. 18) is the point of the maximum in each curve in Fig. 9. At the empirical fleet selectivity, the MSY value is 207.7713kt (Tab. 3), which is close to Kayanda et al. (2009)'s prediction of 212kt and lower than other

380 predictions (Kyomuhendo, 2002; Pitcher and Bundy, 1995). Again, the best scenario is fishing above 50cm, where the maximum sustainable yield is 250.0450kt. Scenario 3 is inferior and scenario 4 has a similar MSY like the open scenario.

For small values of the peak fishing mortality, scenarios 1 and 2 are similar and have a steeper initial slope than scenarios 3 and 4. The reason is that the latter

385 restrict from fishing large fish, which, at the unfished, "pristine" level of the fishing stock, are most abundant and therefore provide high yields. At the other end, for large values of the peak fishing mortality, scenarios 2 and 4 still provide moderate yield levels, because juveniles below 50cm are spared and thus some individuals can still reach maturity and reproduce. Contrarily, in scenarios 1 and 3, juveniles are

390 subject to fishing, which leads, for a high fishing mortality, to fewer survivors very low yields, and eventually the collapse.

An important result is that, under the empirical fleet selectivity, the F_{MSY} value is 1.015230/yr and thus the empirical fishing mortality $F_{emp} = 1.035993/yr$ is only 2.0% above F_{MSY}, which would mean that the fishing levels is close to what is the

395 best level, for the fleet selectivity being as it is. This is different from various other studies, who suggest an overfished, and hence unsustainable, state (e.g. Yongo et al. (2018)), but would explain the relatively stable population of Nile perch in the last decade (LVFO, 2019; Natugonza et al., 2019; Mgaya and Mahongo, 2017; Marshall, 2018). Of course, dynamical factors from the interaction with other species (van

400 Zwieten et al., 2016) or the ecosystem or fluctuations in the fishing level can never

23

be excluded, but at least this single species model hints towards a rather appropriate level of fishing mortality. Improvements in yield could, however, be achieved if the fishing pressure below 50cm were reduced, as scenario 2 suggests. This case is also more stable in the sense that the curvature of the yield curve (Fig. 9) is smaller around the maximum, i.e. the maximum is broader and less sharp which points toward a situation that is more resilient with respect to fluctuations in the level of fishing mortality.

7 Discussion

7.1 Sensitivity analysis

The sensitivity of the model results to the input parameters is evaluated by quantifying the marginal effect of small parameter changes (similar to the suggestion of Pope et al. (2019)). Two model results are considered here as most relevant: The fishing mortality that maximizes yield, F_{MSY}, and the relative recruitment, which denotes the recruitment relative to the maximal possible value, R/R_{max}, which, for simplicity, is in the following also referred to as simply R.

The recruitment is a significant indicator of the state of the fish population. The smaller the value, the greater is the impairment of the stock from fishing. A value of 1 means that there is no impairment at all (unfished case). Limit reference points indicate at which fishing mortality the recruitment is impaired (e.g. at $\frac{R}{R_{max}} = \frac{1}{2}$ as used by Andersen (2019).

We calculate the sensitivity with respect to three parameters: the growth parameter A, the physiological mortality a, and the size at maturation. The first two parameters can only be inferred, but not measured directly. The third parameter can be measured (e.g. Ogutu-Ohwayo (1988)), but the measurement is costly, therefore it is not done frequently.

24

The evaluation is done in two ways: first, the change in absolute values,

- $\frac{\partial R}{\partial q_i}$ for $q_i \in \{A, a, w_{mat}\}$

- $\frac{\partial F_{msy}}{\partial q_i}$ for $q_i \in \{A, a, w_{mat}\}$

and second, the relative change, which can be interpreted as the elasticity of the output variable to the input parameter.

- $\frac{\partial R}{\partial q_i} \Big/ \frac{R}{q_i} = \frac{q_i}{R} \frac{\partial R}{\partial q_i}$

- $\frac{\partial F_{msy}}{\partial q_i} \Big/ \frac{F_{msy}}{q_i} = \frac{q_i}{F_{msy}} \frac{\partial F_{msy}}{\partial q_i}$

The partial derivatives are approximated with the difference quotient using $\Delta q_i = 0.01$, the elasticity with $\Delta q_i/q_i = 1\%$. The basis parameter values are: $A = 13.01879$, $a = 0.3$, $w_{mat} = 4400\ g$. The results are given in Tab. 4. In each column, the largest (absolute) value is marked bold. The largest impact on R comes from the parameter a, both in absolute and relative terms.

Table 4: Relative and absolute sensitivity of R and Fmsy to the parameters A, a and w_{mat}.

parameter	$\frac{\partial R}{\partial q_i}(q_i)$	$\frac{q_i}{R}\frac{\partial R}{\partial q_i}(q_i)$	$\frac{\partial F_{msy}}{\partial q_i}(q_i)$	$\frac{q_i}{F_{msy}}\frac{\partial F_{msy}}{\partial q_i}(q_i)$
A	0.0002967416	0.003807126	0.07798131	**0.9999849**
a	**-0.04937959**	**-0.01384381**	**1.602788**	0.4780612
w_{mat}	2.807272e-07	0.001229598	2.053975e-05	0.08859575

For F_{MSY}, one sees that the elasticity is largest for the parameter A and is approximately one. This means that a faster growing population can tolerate a larger fishing mortality, in almost linear proportion to the growth rate. That implies that it is difficult to estimate both A and F simultaneously from an empirical population spectrum, as a linear scaling of both keeps the spectrum nearly unchanged which was also observed in the numerical simulations (not shown here). In absolute values, the crucial parameter for

F_{MSY} is a where a change of 0.01 in a changes by 0.016/yr. Therefore, in future research the important role of the physiological mortality should be considered.

7.2 Cohort biomass

What is the interpretation of the result that the highest MSY is achieved in the scenario, where all sizes above 50cm are subject to fishing? For this, one has to look at the curve of the cohort biomass (Fig. 10). A cohort is the group of fish that have been born in the same time period (in the continuous case this means fish that are born in the time interval $[t; t + dt]$). The number of fish in a cohort is non-increasing with time, as the only relevant process is mortality which reduces the numbers. The cohort biomass, the sum of the biomass (weight) of all individuals in the cohort, however, has a more complex development. As long as the biomass increase from the growth of the individuals outweighs the biomass loss from mortality, the cohort biomass increases. At some point, typically beyond the maturation size, the mortality becomes so large that it dominates and the cohort biomass decreases. This gives a unimodal curve.

Fig. 10 shows the cohort biomass across the lifespan for the case without fishing. The maximum of the cohort biomass lies at 100.9cm (14318.6g). As Diekert (2012) points out for a similar scenario, under perfect selectivity (i.e. where the target size of fish can be selected with perfect accuracy and precision) the optimal management is to target the fish at the size where the cohort biomass peaks. This means that the perfect management strategy scenario would be to target fish around 100cm - conditional on recruitment being constant. Of the four scenarios, the one where fishing acts above 50cm, is closest to the case of perfectly targeting fish around 100cm as the selectivity is (by design) still not precise, but at least more focused on largest individuals than the other scenarios.
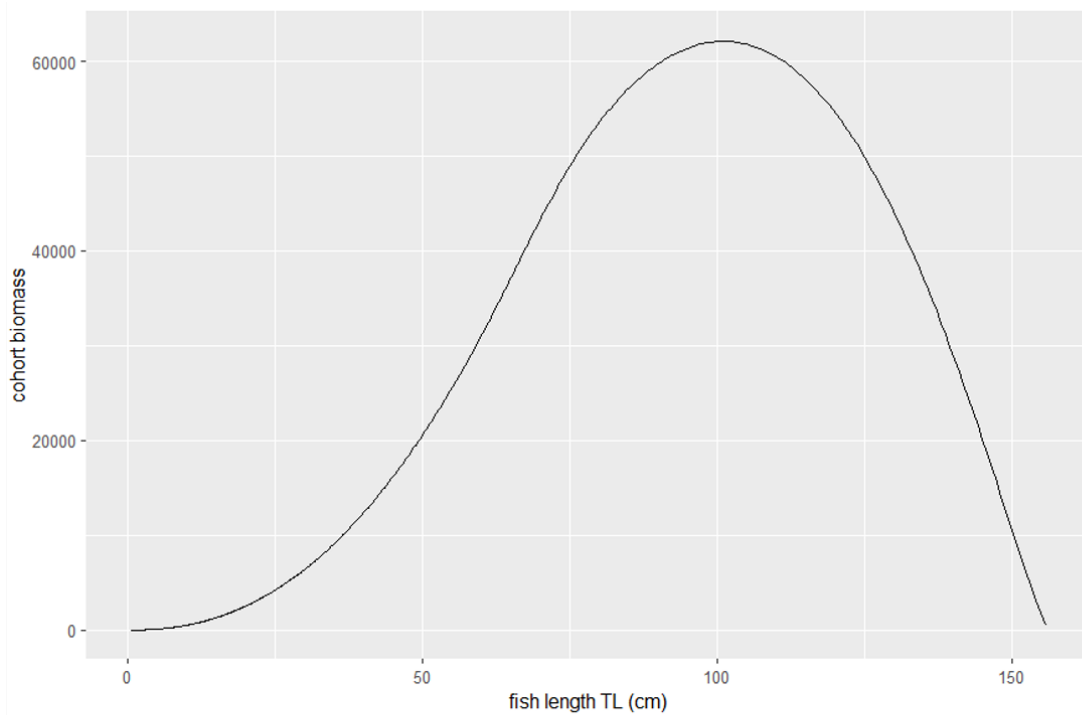
26

Figure 10: Cohort maximum - for a single, isolated species it is identical to optimal knife edge fishing size (for zero costs). Physiological mortality a=0.3.

7.3   Fishing mortality

In the literature, two distinct notion of the term "fishing mortality" are use. Some use the term in the sense of the ratio between annual yield and biomass, or they consider the ratio

470 to be an approximation of the actual fishing mortality (e.g., Natugonza et al. (2019)). It is important to emphasize that this notion is a mortality that is averaged (typically) over time (e.g. one year) and, more importantly average across the population or a major part of it (e.g. all adults). We will refer to this notion as the *annual fishing mortality* as it is, in most cases, calculated from the ratio of the annual yield (catch) to the biomass.

475 The other notion of "fishing mortality" can be found, e.g., in Yongo et al. (2018), where it refers to an *instantaneous rate* and where it can depend, in general, on the size of the fish, this means each size can have a particular mortality rate. This is the notion of mortality rate that is mainly used in this paper. It is important to note that the value

27

of the two notions need not necessarily be the same or not even similar to each other. As the second notion, the *instantaneous rate*, can vary across the fish population, some fish sizes could experience a very low or a very high mortality rate. Therefore, for comparison, the instantaneous rate can translated to an annual mortality by building the ratio of annual catch to biomass. Here, the information how the mortality is distribution across the population, is completely lost. If the fishing mortality is applied equally across the stock and all fish sizes, then the two notions agree. Please note that the mortality that appears in eq. (11)-(18) is the *instantaneous mortality rate*, as can be seen from its use in the McKendrick-von-Foerster equation (eq. 1).

Hence, in the case of the size-structured model used in this paper, the actual fishing mortality rate is not the same for all fish, but depends on the fish size. For the purpose of comparing various fishing levels, therefore, it is helpful to define a reference fishing mortality. In the following this will be the "peak fishing mortality", defined as the instantaneous mortality rate at the size of the maximum of the fleet selectivity curve, with the unit 1/yr.

To compare the results to estimates of the fishing mortality from the literature, the following approach is used. Across the range of admissible peak fishing mortality values, from F=0 to the point where the stock collapses at $F_{crash} = 5.52/yr$, the ratio between annual yield and the stock biomass is calculated. This ratio, equivalent to the widely used first definition of fishing mortality, and the peak fishing mortality are in direct relation to each other - and the mapping between the two quantities is unique in the range of admissible peak fishing mortality values. This means that the conductor of a survey, when he would observe the simulated stock in the reality, would interpret this yield/biomass ratio as the fishing mortality, if he uses the respective definition of biomass. Because of the 1-to-1 mapping, the peak fishing mortality rates of the model simulations can uniquely be

28

compared to conventional fishing mortality values. The mapping is shown in Fig. 11.
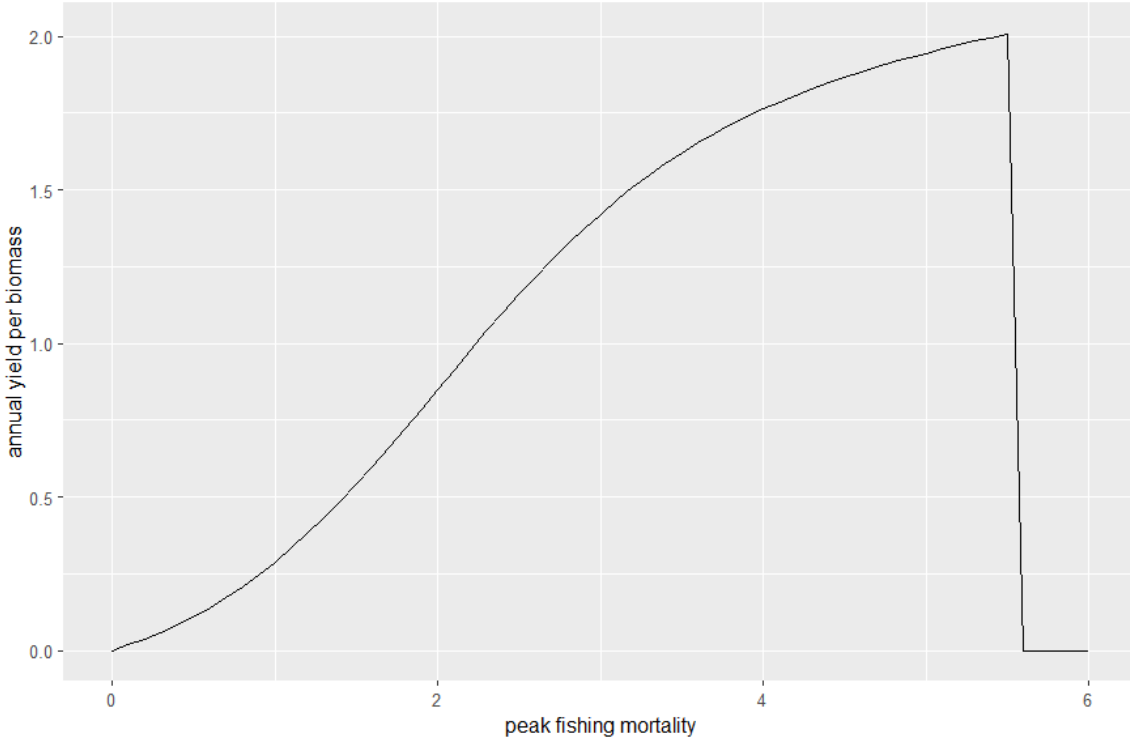

Figure 11: The relationship between the peak fishing mortality (an instantaneous mortality rate) and the annual fishing mortality (yield per biomass). The stock collapses at $F_{crash} = 5.52/yr$.

With the mapping, the result of this paper - the value of F_{MSY} under the current fleet selectivity, $F_{MSY} = 1.01523/yr$ - can be compared to empirical estimates from the literature and to other model simulations. In simulations of two models with biomass flux balances, Natugonza et al. (2019) finds - using definition (1) - a fishing mortality of $0.312/yr$ (Atlantis) and $0.340/yr$ (EwE), respectively. Using the relationship, this corresponds to a peak fishing mortality of $1.05/yr$ and $1.11/yr$, respectively, similar to the finding of this paper, $F_{MSY} = 1.01523/yr$. From an empirical analysis of commercial catch samples from two Kenyan landing sites, Yongo et al. (2018) estimate a fishing mortality of $0.54/yr$, corresponding to a peak fishing mortality of $1.50/yr$, somewhat higher than our finding. However, the value $1.50/yr$ might be not fully accurate, as it was derived only from catch

29

samples and not from the actual population in the lake whose size structure obviously

515 differs systematically, due to the selectivity of the fishery.

7.4   Physiological mortality

The previous subsection has shown that the parameter of the physiological mortality, a,

plays a crucial role for the recruitment and F_{MSY}. As the parameter cannot be directly

measured, the following section shows how the model simulations compare to the bottom-

520 trawl measurement for four values of a: 0.2, 0.3, 0.4, 0.5. These values were selected to

represent approximately the range of likely a-values (see appendix, "Physiological mortal-

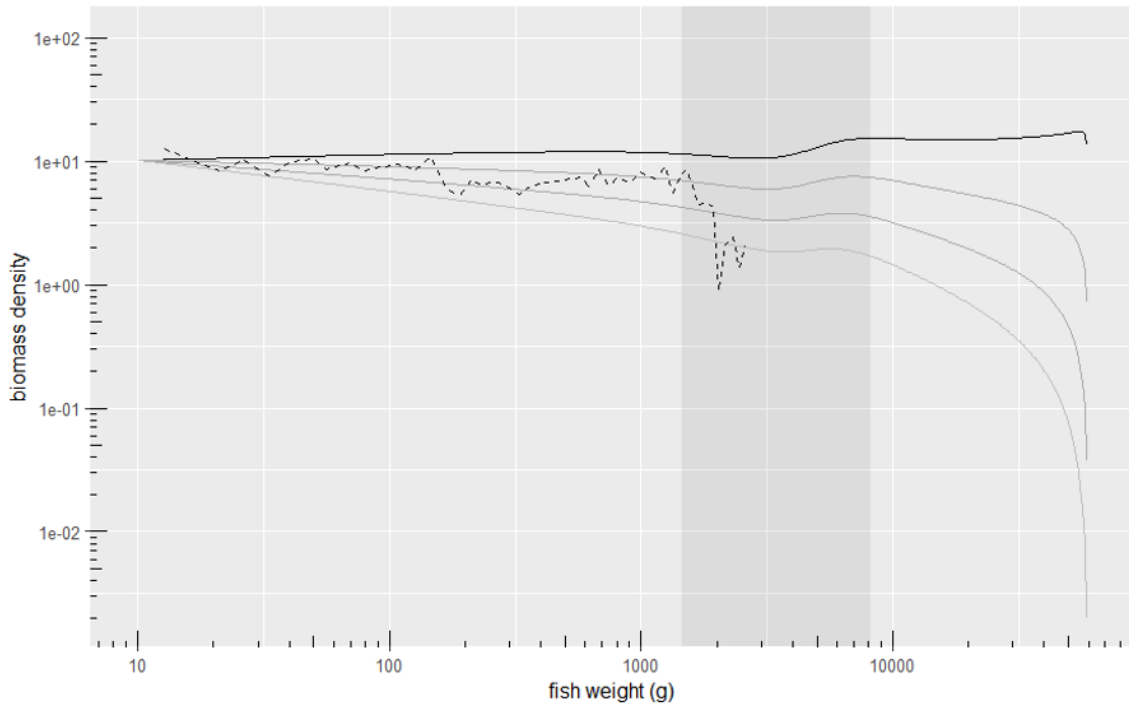ity"). The result of the four simulations is given in Fig. 12.

Figure 12: The spectrum as calculated from the model for F=0.5 with the physi-
ological mortality a=0.2 to a=0.4 from black to grey, together with the data from
the bottom trawl survey 2019 (dashed).

The curve of the empirical spectrum measurements lies in the range that is spanned

by the four simulations. In the beginning, between around 10 to 100g, the empirical curve

30

follows closely the simulation of $a = 0.3$. Between 100g and 1000g, it lies between the curves of $a = 0.3$ and $a = 0.4$. Beyond 1000g, approximately at 50cm (grey shaded area in Fig. 12), the empirical curve drops. This can be related to a decreased selectivity as discussed previously, therefore this part of the curve has lower confidence. From the comparison it is concluded that it is likely that a is around 0.3-0.4 which agrees with the theoretical expectation. From an optimization that minimizes the sum of squared residuals, the optimal fit to the bottom-trawl spectrum turns out to be a simulation with a=0.3278.

Table 5: The slopes are calculated from a linear regression of the biomass spectrum in the range 10-50cm (7.6g-1451.7g) in a double-logarithmic setting, corresponding to a powerlaw function $B(w) = w^s + C$ with slope s and a constant C. Sim are the model simulations, BT2019 is the bottom-trawl survey of 2019.

data set	a	slope s	R2 (adjusted)	p value	data points
Sim	0.2	0.03414±0.00066	0.9005	< 2.2e-16 ***	291
Sim	0.3	-0.06586±0.00066	0.9711	< 2.2e-16 ***	291
Sim	0.4	-0.16586±0.00066	0.9953	< 2.2e-16 ***	291
Sim	0.5	-0.26586±0.00066	0.9982	< 2.2e-16 ***	291
BT2019		-0.09878±0.01925	0.4063	1.007e-05 ***	36

The slope of the size spectrum is directly related to the parameter a which can be seen from the analytical solution of eq. (11) for appropriate μ-functions. For the four simulations of the previous section (a=0.2, 0.3, 0.4, 0.5) and the bottom-trawl spectrum, the slope values of the biomass spectrum in the range 10cm-50cm (7.6g-1451.7g) have been calculated. The results are shown in Tab. 5. The slope is 0.03414 in the simulation with $a = 0.2$ and decreases by 0.1 with each increment in a. For the bottom-trawl survey, the slope is -0.09878, which is between the slopes of the simulations for 0.3 and 0.4 which agrees with the findings from the previous section.

8 Conclusion

We have applied the modelling framework of Andersen (2019) to build a size structured model of the Nile perch fishery at Lake Victoria. The model was used to understand the effect of the size selectivity of the fishery, and, with it, the potential of size-based policies. The model was validated by comparing the emergent simulated growth curve with the well-known van Bertalanffy curve and by comparison to the size structure from three different surveys.

Using the empirical fleet selectivity from Gómez-Cardona et al. (2022) as an input into the model, the simulations of the size structure of the fish population, in equilibrium with fishing, are similar to the empirical size distribution from the bottom-trawl and the catch assessment survey. The size distribution of the hydroacoustic survey, however, differs both from the bottom-trawl survey and from the model simulation. Therefore we conclude that it is more likely that the hydroacoustic survey does not represent the size structure correctly. A potential reason could be the target strength-size relation in the calibration of the hydroacoustic survey, but more research is needed to investigate the cause.

We find that, under the current fleet selectivity, the empirical annual yield (207.5936kt) is close to the maximum sustainable yield (207.7713kt). Correspondingly, also the empirical peak fishing mortality rate, F=1.035993/yr, is only 2.0% above the rate that leads to the maximum sustainable yield (F=1.015230/yr). The value of MSY is similar to the previous estimate of Kayanda et al. (2009).

In addition to the empirical selectivity of the fishery we have simulated three hypothetical fleet selectivity shapes to predict the effect of the selectivity on the fish stock and the equilibrium yield. For the comparison, each scenario was simulated as the solution of the steady state of the McKendrick-von-Foerster equation across a wide range of fishing levels.

32

₅₆₅ We find that sparing all fish below 50cm, while keeping the fishing mortality above 50cm the same, increases the annual yield by 17.7.% from 207.5936kt to 244.302kt. Catching no fish above 85cm, decreases yield by -28.0% from 207.5936kt to 149.5158kt. The maximum sustainable yield is highest in the scenario where fishing is only above 50cm, and lowest in the scenario where fishing is only below 85cm.

₅₇₀ We have tested the sensitivity of the results and have found that the parameter of physiological mortality, which represents natural mortality, plays the most important role. The value of the growth parameter and of the maturation size have less influence on the results.

While this study does not raise the claim to describe fishers' reaction to size regulations, ₅₇₅ it provides a study of the effect of one empirical and three hypothetical selectivities on the fish stock and the yield and therefore provides an understanding of the relationship between the fleet selectivity and the equilibrium yield. While our study indicates that the empirical yield is close to the maximum sustainable yield, it depicts the significant potential improvement in annual yield that could emerge from reducing the fishing pressure ₅₈₀ on juvenile fish below 50cm.

9 Appendix

9.1 Length to weight conversion

A fish population can be represented with a length spectrum or a weight spectrum. The number spectrum can be converted between the two representations from the following considerations. Let $n_L(L)$ denote the number density in the length spectrum, such that the number of fish in the interval $[L_1, L_2]$ is:

$$N = \int_{L_1}^{L_2} n_L(L)dL \tag{21}$$

This number does not differ from the one in the weight representation:

$$N = \int_{w(L_1)}^{w(L_2)} n_w(w)dw \tag{22}$$

where w(L) denotes the length-weight relation, and $n_w(w)$ is the number density of the weight spectrum. As the equations are true for any pair L_1, L_2 and the respective pair $w(L_1), w(L_2)$, it holds that

$$n_L(L)dL = n_w(w)dw \tag{23}$$

or

$$n_w(w) = n_L(L)(\frac{dw}{dL})^{-1} \tag{24}$$

where

$$\frac{dw}{dL} = \frac{d}{dL}w(L) = cbL^{b-1} \tag{25}$$

34

is the derivative of the length-weight-relation

$$w(L) = cL^b \tag{26}$$

which is commonly applied in fisheries sciences.

Hence the density conversions is:

$$n_w(w) = n_L(L)(cbL^{b-1})^{-1} \tag{27}$$

and, analogously:

$$n_L(L) = n_w(w)bc^{1/b}w^{(b-1)/b} \tag{28}$$

where we used the inverse length-weight relation $L(w) = (w/c)^{1/b}$ and its derivative $\frac{dL(w)}{dw} = bc^{1/b}w^{(b-1)/b}$.

This length-to-weight conversion was validated against the method LBNbiom using the logarithmically binned biomass (Edwards et al., 2017).

9.2   Growth parameter

Andersen (2019 Fish Ecology; p. 43, eq. (3.10)) describes how the growth parameter A can be estimated from the Bertalanffy parameters K and L_∞ for n=3/4 and b=3. We extend the derivation for arbitrary values of n and b. From the length-weight relationship

$$w = cL^b \tag{29}$$

it follows that

$$\frac{dL}{dt} = \frac{1}{b}c^{-1/b}w^{1/b-1}\frac{dw}{dt} \tag{30}$$

35

Inserting the van Bertalanffy equation

$$\frac{dL}{dt} = KL_\infty \tag{31}$$

and the juvenile growth model

$$\frac{dw}{dt} = Aw^n \tag{32}$$

one gets

$$KL_\infty = \frac{A}{b}c^{-1/b}w^{1/b-1+n} \tag{33}$$

Following Andersen (2019), let us assume the two are identical at $w = w_m = \eta_m W_\infty = \eta_m cL_\infty{}^b$. Then

$$KL_\infty = \frac{c^{-1/b}}{b}(\eta_m cL_\infty{}^b)^{1/b-1}A(\eta_m cL_\infty{}^b)^n \tag{34}$$

Therefore:

$$A = bc^{1-n}\eta_m{}^{1-1/b-n}KL_\infty{}^{b(1-n)} \tag{35}$$

For n=3/4 and b=3 one gets the special case shown in eq. (3.10) of Andersen (2019):

$$A = 3c^{1/4}\eta_m{}^{-1/12}KL_\infty{}^{3/4} \tag{36}$$

With the standard parameter values (Tab. 1) one gets A=13.02.

9.3   Physiological mortality

Andersen (2019) describes two different ways to calculate the parameter a which represents the physiological mortality (p. 77, eq. 4.41 and 4.42). The first method builds on the size spectrum theory and the energy budget. From the predator-prey interactions in the

36

marine size spectrum and the metabolism, the physiological mortality a is:

$$a = a(\beta, \sigma, n, q, f_0, \epsilon_a, f_C) = \frac{\Phi_p f_0}{\epsilon_a(f_0 - f_c)} \tag{37}$$

where

$$\Phi_p = \beta^{2n-q-1} exp((2n - q - 1)(q - 1)\sigma^2/2) \tag{38}$$

comes from the feeding kernel for a community spectrum.

With the standard parameter values (Tab. 1) one gets a=0.522.

The advantage of this approach is that is derived from very general principles and thus applies broadly, the disadvantage is that there are no direct observations of q, f_0, ϵ_A, f_c. Therefore general species-unspecific and not directly observable values have to be used.

The second method to estimate a is from empirical observations of M and K with the advantage of using species-specific values which are often measured or estimated in the literature and having the parameter K from the van Bertalanffy curve. However, as the natural mortality depends on the weight, M is not actually a constant. Therefore, one has to set, rather arbitrarily, a weight at which the size-based natural mortality equals M. Following Andersen (2019) in setting this point at the size of maturation, one gets:

$$a = a(M, K, \eta_m, b) = \frac{M}{K} \frac{\eta_m^{1/b}}{b} \tag{39}$$

With the standard parameter values (Tab. 1) one gets a=0.244.

9.4 van Bertalanffy growth curve

This is the length-at-age curve with (1) the van Bertanlanffy equation and (2) the integration of the biphasic growth model. Partly, the difference comes from the fact that in the van Bertalanffy equation, fish start at $t = 0$ with a positive weight due to the negative value of "age at zero lenght", t_0.
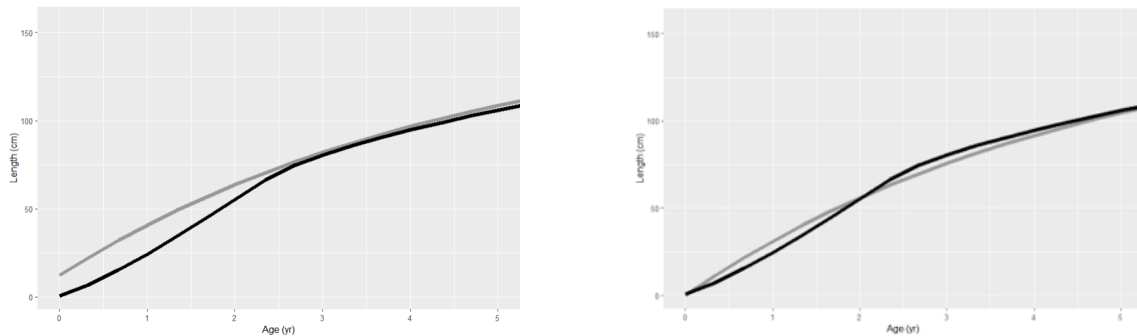

Figure 13: Van Bertalanffy growth curve (grey) vs integration of the differential equation dw/dt with biphasic growth (black). The left figure uses $t_0 = -0.37yr$ (fishbase.se, 2022), the right figure $t_0 = 0$.

References

Andersen, K. (2020). Size-based theory for fisheries advice. *ICES Journal of Marine Science*, 77(7-8):2445–2455.

Andersen, K. H. (2019). *Fish Ecology, Evolution, and Exploitation: A New Theoretical Synthesis*, volume 93. Princeton University Press.

Andersen, K. H., Jacobsen, N. S., and van Denderen, P. D. (2019). Limited impact of big fish mothers for population replenishment. *Canadian Journal of Fisheries and Aquatic Sciences*, 76(3):347–349.

Aura, C. M., Nyamweya, C. S., Owili, M., Gichuru, N., Kundu, R., Njiru, J. M., and Ntiba, M. J. (2020). Checking the pulse of the major commercial fisheries of lake victoria kenya, for sustainable management. *Fisheries Management and Ecology*, 27(4):314–324.

Barneche, D. R., Robertson, D. R., White, C. R., and Marshall, D. J. (2018). Fish reproductive-energy output increases disproportionately with body size. *Science*, 360(6389):642–645.

Brierley, A. (2018). Poaching lake victoria's fish for traditional chinese medicine. *Nature*, 553(7686):27–28.

Christensen, V. and Walters, C. J. (2004). Ecopath with ecosim: methods, capabilities and limitations. *Ecological modelling*, 172(2-4):109–139.

Diekert, F. K. (2012). Growth overfishing: the race to fish extends to the dimension of size. *Environmental and Resource Economics*, 52(4):549–572.

Downing, A. S., Galic, N., Goudswaard, K. P., van Nes, E. H., Scheffer, M., Witte, F., and Mooij, W. M. (2013a). Was lates late? a null model for the nile perch boom in lake victoria. *PloS one*, 8(10).

660 Downing, A. S., Van Nes, E. H., Janse, J. H., Witte, F., Cornelissen, I. J., Scheffer, M., and Mooij, W. M. (2012). Collapse and reorganization of a food web of mwanza gulf, lake victoria. *Ecological Applications*, 22(1):229–239.

Downing, A. S., van Nes, E. H., van de Wolfshaar, K. E., Scheffer, M., and Mooij, W. M. (2013b). Effects of resources and mortality on the growth and reproduction of nile perch
665 in lake victoria. *Freshwater Biology*, 58(4):828–840.

Echoview Software Pty Ltd. (2016). Echoview version 8.0. hobart, australia (8.0). *Echoview Software Pty Ltd.*

Edwards, A. M., Robinson, J. P., Plank, M. J., Baum, J. K., and Blanchard, J. L. (2017). Testing and recommending methods for fitting size spectra to data. *Methods in Ecology*
670 *and Evolution*, 8(1):57–67.

fishbase.se (2022). Life history data on lates niloticus. `https://www.fishbase.se/popdyn/KeyfactsSummary_1.php?ID=347&GenusName=Lates&SpeciesName=niloticus&vStockCode=361&fc=631`.

Gómez-Cardona, S., Kammerer, J., and Mrosso, H. (2022). Fishing fleet selectivity in lake
675 victoria's nile perch fishery. *AWI discussion paper series*.

Kayanda, R., Everson, I., Munyaho, T., and Mgaya, Y. (2012). Target strength measurements of nile perch (lates niloticus: Linnaeus, 1758) in lake victoria, east africa. *Fisheries Research*, 113(1):76–83.

Kayanda, R., Taabu, A. M., Tumwebaze, R., Muhoozi, L., Jembe, T., Mlaponi, E., and
680 Nzungi, P. (2009). Status of the major commercial fish stocks and proposed species-specific management plans for lake victoria. *African Journal of Tropical Hydrobiology and Fisheries*, 21:15–21.

40

Kolding, J., Van Zwieten, P., Mkumbo, O., Silsbe, G., and Hecky, R. (2008). Are the lake victoria fisheries threatened by exploitation or eutrophication? towards an ecosystem based approach to management. *The ecosystem approach to fisheries*, pages 309–354.

Kyomuhendo, P. (2002). A bioeconomic model for uganda's lake victoria nile perch fishery. Master's thesis, Universitetet i Tromsø.

LVFO (2016). Regional catch assessment survey synthesis report, june 2005 to november/december 2015. *LVFO*.

LVFO (2017). Regional status report on lake victoria bi-ennial frame surveys between 2000 and 2016. *Regional Frame Survey Report*.

LVFO (2019). A report of the lake-wide hydroacoustic survey. *Hydro-acoustics Regional Working Group*.

Marshall, B. E. (2018). Guilty as charged: Nile perch was the cause of the haplochromine decline in lake victoria. *Canadian Journal of Fisheries and Aquatic Sciences*, 75(9):1542–1559.

McKendrick, A. (1925). Applications of mathematics to medical problems. *Proceedings of the Edinburgh Mathematical Society*, 44:98–130.

Mgaya, Y. D. and Mahongo, S. B. (2017). Lake victoria fisheries resources. *Springer*.

Natugonza, V., Ainsworth, C., Sturludóttir, E., Musinguzi, L., Ogutu-Ohwayo, R., Tomasson, T., Nyamweya, C., and Stefansson, G. (2019). Ecosystem models of lake victoria (east africa): Can ecopath with ecosim and atlantis predict similar policy outcomes? *Journal of Great Lakes Research*.

Natugonza, V., Ogutu-Ohwayo, R., Musinguzi, L., Kashindye, B., Jónsson, S., and Valtysson, H. T. (2016). Exploring the structural and functional properties of the lake victoria

41

food web, and the role of fisheries, using a mass balance model. *Ecological modelling*, 342:161–174.

Njiru, M., Getabu, A., Taabu, A. M., Mlaponi, E., Muhoozi, L., and Mkumbo, O. (2009). Managing nile perch using slot size: is it possible? *African Journal of Tropical Hydro-biology and Fisheries*.

Nyamweya, C., Kisumu, K., and Thordarson, G. (2012). *Modelling and forward projections of Nile perch, Lates niloticus, stock in Lake Victoria using GADGET framework*. PhD thesis, Thesis, United Nations University of the Fisheries Training Progremme.

Ogutu-Ohwayo, R. (1988). Reproductive potential of the nile perch, lates niloticus l. and the establishment of the species in lakes kyoga and victoria (east africa). *Hydrobiologia*, 162(3):193–200.

Perivolioti, T.-M., Frouzova, J., Tušer, M., and Bobori, D. (2020). Assessing the fish stock status in lake trichonis: A hydroacoustic approach. *Water*, 12(6):1823.

Pitcher, T. J. and Bundy, A. (1995). Assessment of the nile perch fishery in lake victoria. In *The impact of species changes in African lakes*, pages 163–180. Springer.

Pope, J. G., Bartolino, V., Kulatska, N., Bauer, B., Horbowy, J., Ribeiro, J. P., Sturlu-dottir, E., and Thorpe, R. (2019). Comparing the steady state results of a range of multispecies models between and across geographical areas by the use of the jacobian matrix of yield on fishing mortality rate. *Fisheries Research*, 209:259–270.

van de Wolfshaar, K. E., HilleRisLambers, R., Goudswaard, K. P., Rijnsdorp, A. D., and Scheffer, M. (2014). Nile perch (lates niloticus, l.) and cichlids (haplochromis spp.) in lake victoria: could prey mortality promote invasion of its predator? *Theoretical ecology*, 7(3):253–261.

van Zwieten, P. A., Kolding, J., Plank, M. J., Hecky, R. E., Bridgeman, T. B., MacIntyre, S., Seehausen, O., and Silsbe, G. M. (2016). The nile perch invasion in lake victoria: cause or consequence of the haplochromine decline? *Canadian Journal of Fisheries and Aquatic Sciences*, 73(4):622–643.

von Foerster, H. (1959). Some remarks on changing populations. *The Kinetics of Cellular Proliferation, Grune and Stratton*, pages 382–407.

Yongo, E., Agembe, S., Outa, N., and Owili, M. (2018). Growth, mortality and recruitment of nile perch (lates niloticus) in lake victoria, kenya. *Lakes & Reservoirs: Research & Management*, 23(1):17–23.